



Eidgenössische Technische Hochschule Zürich
Swiss Federal Institute of Technology Zurich

QUANTUM DEVICE LAB

SEMESTER THESIS

Investigating High Repetition Rates for a Metastable Helium Source

BY ALISHA DÜTSCHLER

Supervisor:
Dr. Sébastien GARCIA

Principal Investigator:
Prof. Dr. Andreas WALLRAFF

October 6, 2017

Abstract

So far the Rydberg experiments repetition rate was limited to 25 Hz. In this thesis we will discuss a new setup which can be used with repetition rates of around 1 kHz. Tests of this setup with repetition rates up to 500 Hz were conducted and will be presented.

Contents

1	Introduction	2
1.1	Qubits and quantum information processing	2
1.2	The Rydberg experiment	2
1.3	Setup of the main experiment	3
1.4	Excitation of Helium to Rydberg levels	4
1.5	Increasing the repetition rate	4
2	Experimental setup	6
2.1	Metastable helium source	6
2.2	Micro-channel Plate	7
2.3	Camera program and properties	8
3	Results	9
4	Conclusion and outlook	14
	References	16
A	LabVIEW Camera Driver Manual for UBS 3 CMOS Camera	17

1 Introduction

1.1 Qubits and quantum information processing

In classical computing information is stored in bits. These bits can each be in one of two possible distinct states. In quantum computing however a qubit, the quantum equivalent of the classical bit, can also be in a superposition of these two states. There exist several different realizations of such a qubit. The two examples which are most interesting for us are superconducting qubits and Rydberg atoms. The advantage of superconducting qubits is their fast processing rate and scalability, however they have short coherence times. Rydberg atoms are atoms where the outermost electron has a very high principal quantum number n . The core is shielded by the inner electrons and Rydberg atoms can be treated in the same way as the hydrogen atom in quantum mechanics. The goal is to develop a hybrid system where Rydberg atoms couple to the microwaves emitted by superconducting qubits in a microwave cavity. One could then profit from the large coherence time of Rydberg atoms. Another reason for the use of Rydberg atoms is their large transition dipole moment and therefore their strong coupling to the electric microwave field.

Rydberg atom do not only have transitions in the microwave regime but also in the optical regime. Rydberg atoms could therefore further be used to convert microwave information into optical information.

1.2 The Rydberg experiment

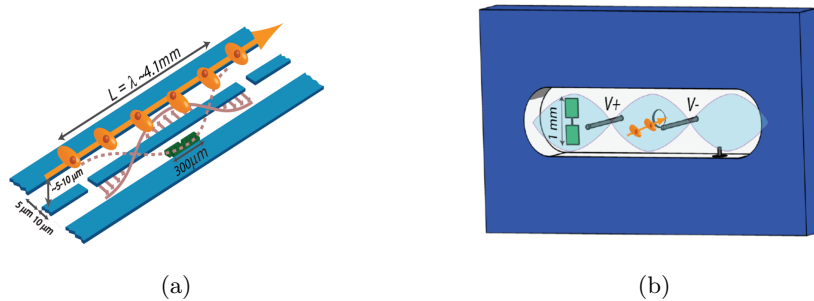


Figure 1: (a) CPW resonator coupling scheme of Rydberg atoms to superconducting qubits. (b) 3D cavity coupling scheme. Rydberg atoms are marked in orange and a transmon qubit green.

The goal of the Rydberg experiment is to couple Rydberg atoms to superconducting qubits through microwave photons. This could be done with a 2 D or a 3 D approach. Figure 1a shows how this can be done in 2 D. Rydberg atoms (orange) pass close over the surface of a coplanar waveguide resonator. The Rydberg atoms couple to the microwave photons (brown). The transmon qubit (green) also couples to the microwave photons. In 3 D the Rydberg atoms (orange) pass through the cavity in which a transmon qubit is placed. This is shown in figure 1b.

The first step in realising this hybrid setup is to measure the coupling of Rydberg atoms to microwave cavities. Due to their low energies the microwave photons are difficult to detect. We therefore need a large dataset over which we can average to reduce noise. Hence high repetition rates are crucial. We now present the setup of the main experiment and what limits we have on the repetition rate. We then see how this is improved in the new setup.

1.3 Setup of the main experiment

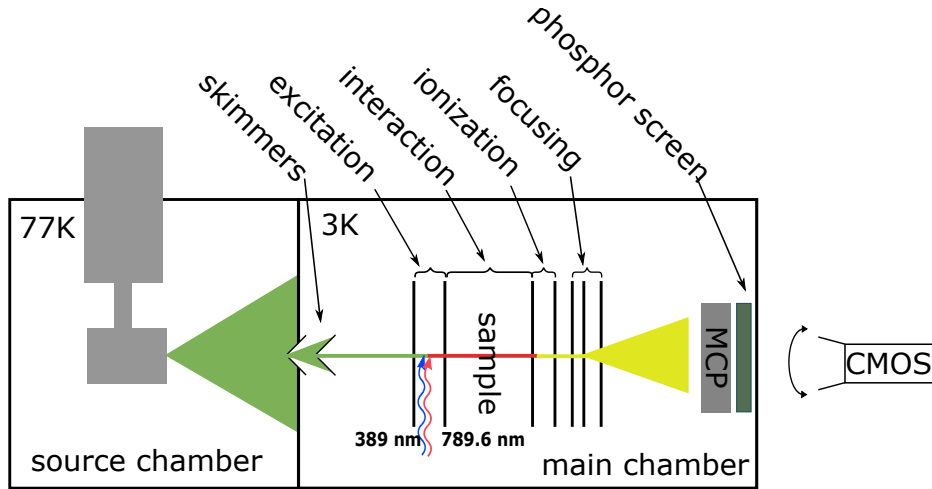


Figure 2: Schematic of the experimental setup. The metastable helium atoms (He^*) released into the source chamber are marked in green. They pass into the main chamber and are excited into Rydberg states (red). The yellow beam represents electrons. The electrons are then detected with a MCP, a phosphor screen and a camera.

In this section we describe the setup of the main Rydberg experiment. A more detailed description of this can be found in [1]. The data presented in this thesis however was obtained on a newer setup. This setup is slightly different and is discussed in [2].

A schematic of the setup can be seen in figure 2. The experiment can be divided into two parts the source chamber and the main chamber. In the source chamber the helium source, marked in grey in figure 2, releases pulses of helium atoms into the source chamber where they undergo supersonic expansion. A dielectric discharge excites the helium atoms into metastable helium He^* (green). Through two skimmers the metastable helium atoms pass into the main chamber. Between the first two electrodes they are excited into the Rydberg state. The Rydberg atoms then interact with the sample and later are ionized between two more electrodes. The electrons (yellow), which were separated from the Helium nuclei, are then focused with three more electrodes in an Einzel lens configuration. The electrons then enter the multi channel plate (MCP) get multiplied and then hit the phosphor screen. The camera then takes images of the phosphor screen.

1.4 Excitation of Helium to Rydberg levels

In this section we explain how Helium is excited into Rydberg states. The involved energy levels are shown in figure 3. The Helium first has to be excited into a metastable state with a dielectric discharge. So far they were excited into the singlet state 2^1S_0 . Then a pulsed UV laser (313 nm) is used to excite them into the singlet Rydberg state $n^1\text{P}_1$. The pulsed laser however limits the repetition rate to 25 Hz.

In our setup they are now excited into the metastable triplet state 2^3S_1 . Then we have a two photon excitation into the triplet Rydberg state $n^3\text{S}_1$ via the 3^3P_0 state. This is done with a blue laser (389 nm) and an infrared laser with a wavelength of 789.6 nm. Both lasers are continuous wave lasers and we use an acousto-optic modulator to pulse the intensity. Therefore we no longer have the limitation on the repetition rate from the laser system.

1.5 Increasing the repetition rate

The use of a pulsed laser to excite the metastable Helium atoms into a Rydberg state limits the repetition rate of the whole main experiment. With the new laser excitation scheme we can go to much higher repetition rates

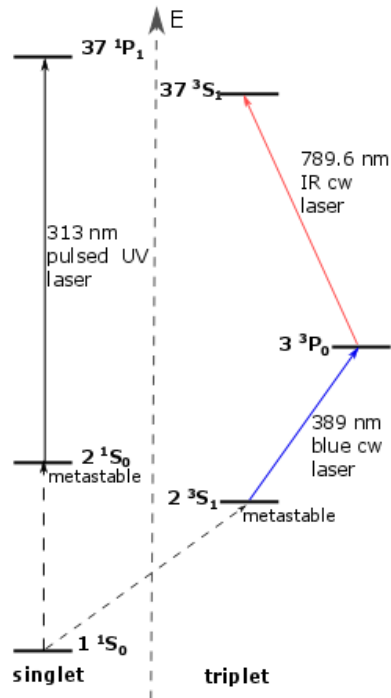


Figure 3: Energy levels of Helium in singlet (left) and triplet (right) states. Excitation to metastable state(dashed arrows) is achieved by dielectric barrier discharge. Excitation to the singlet Rydberg state in the main experiment is done with a pulsed UV laser. In the new setup there is a two photon excitation with a blue and an IR continuous wave laser into the triplet Rydberg state. (Not shown to scale.)

due to the use of continuous wave lasers and an acousto-optic modulator.

Now this issue is solved we needed a new source which can produce metastable Helium at higher repetition rates. This source is described in 2.1. In section 3 we then present the measured properties of the metastable atom beam produced by the new source. In section 2.2 the MCP setup is explained.

To keep up with the higher repetition rates we also used a new camera. In the course of this semester project we have written a camera driver which is described in section 2.3 and the appendix A.

2 Experimental setup

In this section parts of the setup of the new experiment are explained. This setup was then used for the acquisition of the data presented in the next section. First we describe the helium source, then the MCP and finally the camera.

2.1 Metastable helium source

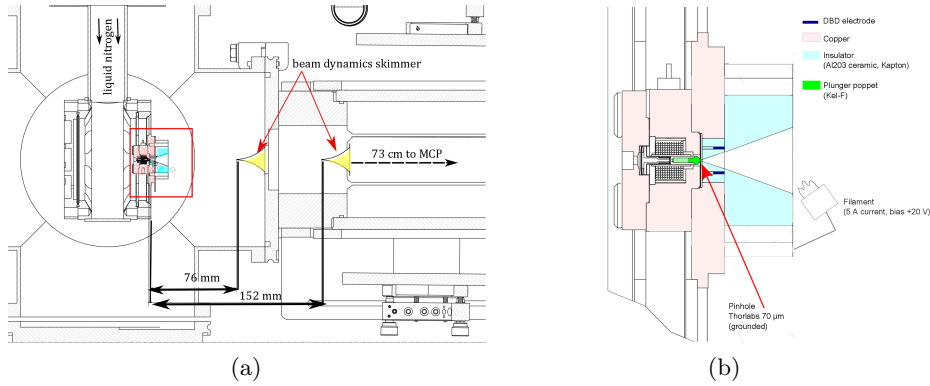


Figure 4: Schematic of the helium source. (b) shows a close up of the region marked in red.

Figure 4a shows a schematic of the setup used for this thesis in the source chamber. In Figure 4b a close-up of the area marked in red is shown. The plunger poppet (green) is retracted when a current flows through the wire around the magnetic plunger. Helium gas can then exit through the pinhole ($75 \mu\text{m}$) into the source chamber. The pinhole is much smaller than in the main setup (0.51 mm [1]). A certain threshold density is needed to produce the plasma in between the dielectric barrier discharge (DBD) electrodes. Because of the smaller pinhole a smaller gas-load is needed to achieve the same density. This has the advantage that the pressure in the source chamber will increase less. Between the DBD electrode (dark blue) part of the helium is excited into a metastable state (He^*). It then continues its supersonic expansion. Attached to the source is also a filament. A 5 Ampere current on the filament seeds the Helium discharge with electrons. Manually liquid nitrogen can be poured into the source. This reduces the speed of the helium atoms. They then move at $\sim 900 \text{ m s}^{-1}$. Cooling would therefore lead to longer interaction times of the Rydberg atoms with a sample.

The current used to open the valve is typically in the range of 40 – 50 A. The valve is also operated with a voltage of 35 – 45 V. Typical pulse lengths are 10 – 20 μs . The discharge is switched on with delays of 40 – 50 μs and a control voltage of ~ 150 V.

2.2 Micro-channel Plate

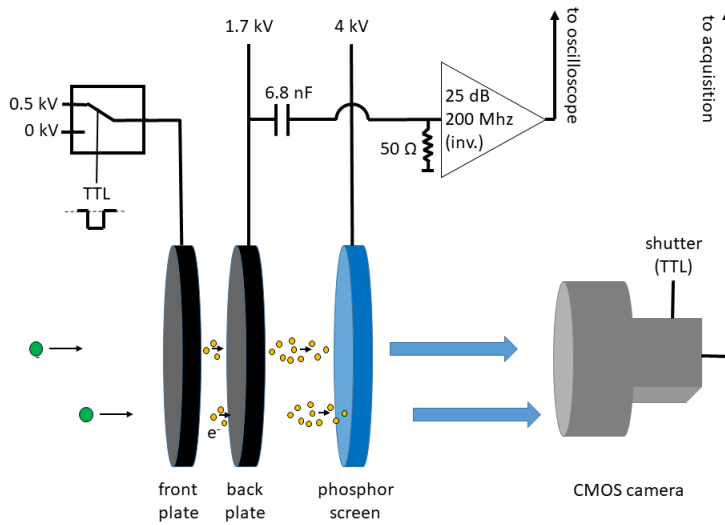


Figure 5: Sketch of the MCP setup. Incoming particles hitting the front plate of the MCP produce an avalanche of electrons. These are accelerated towards the back plate and produce more electrons. These electrons are further accelerated towards the phosphor screen. A camera can then take images of the phosphor screen. The voltage drop on the back plate is amplified and sent to an oscilloscope.

The micro-channel plate (MCP) we use in this experiment has a diameter of 40 mm with channel diameters of 10 μm . The channels form an angle of 8° with the surface normal. We use a MCP in Chevron configuration. That means that we have two plates, where the channels in the second one are rotated in the opposite direction. A particle (e.g. electron, He^* , ion) with a large enough energy hits the wall of a channel of the first (front) plate and secondary electrons are emitted from the dielectric coating. Due to the potential difference the electrons are accelerated and create even more electrons.

From a single incident particle we get an avalanche of around 10^7 electrons [3].

The voltage drop on the back plate is capacitively sent to the oscilloscope after amplification. This allows us to monitor the arrival time of the particles. Behind the back plate a phosphor screen is positioned.

The data presented in later chapters was acquired with 1.7 kV on the back plate and 4.0 kV on the phosphor screen. A voltage of 0.5 kV is constantly applied to the front plate. The potential difference between the front and the back plate however then is not large enough. A switch applies a voltage of 0 kV to the front when we want to detect the incoming particles. This is done to reduce ageing of the MCP. Every particle hitting the MCP damages the dielectric coating of the channels. The accumulation of charge leads to gain degradation.

2.3 Camera program and properties

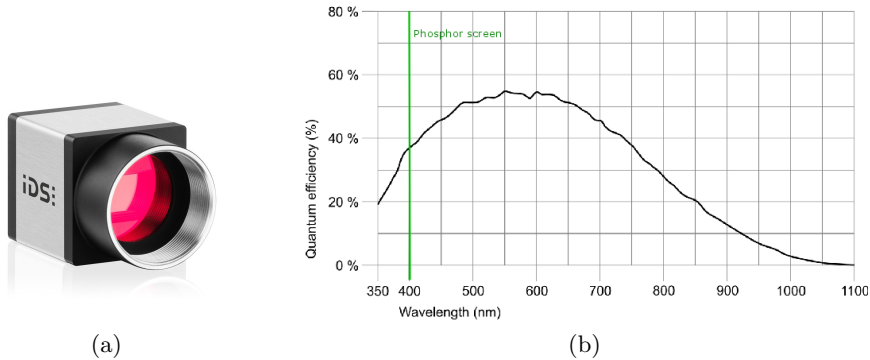


Figure 6: Camera IDS UI-3140CP-M-GL Rev.2 :(a) Camera. (b) Quantum efficiency is shown. In green the characteristic wavelength of the phosphor screen is marked. Figures adapted from camera documentation [4]

We use an IDS UBS 3 CMOS Camera to take pictures of the phosphor screen. That way we also get spatial information about the incoming electrons. The camera model is UI-3140CP-M-GL Rev.2 and is shown in figure 6a. This camera model was chosen for its relatively high frame rate (224.0 fps [4]). This can further be increased by subsampling the image or by reducing the

area of interest. The camera also has a good detection at the characteristic wavelength of the phosphor screen. This is depicted in 6b.

The camera can be controlled with a LabVIEW Camera Driver written as part of this semester thesis. The camera can be triggered externally or with a software trigger. Either way a number of pictures is taken, they are averaged and then displayed. They can also be saved if desired. It is also possible to take a background image and subtract it from the the images. This is needed if we want to compare the results for different repetition rates. The camera driver and the functionality of the SubVis are explained in more detail in the appendix A.

3 Results

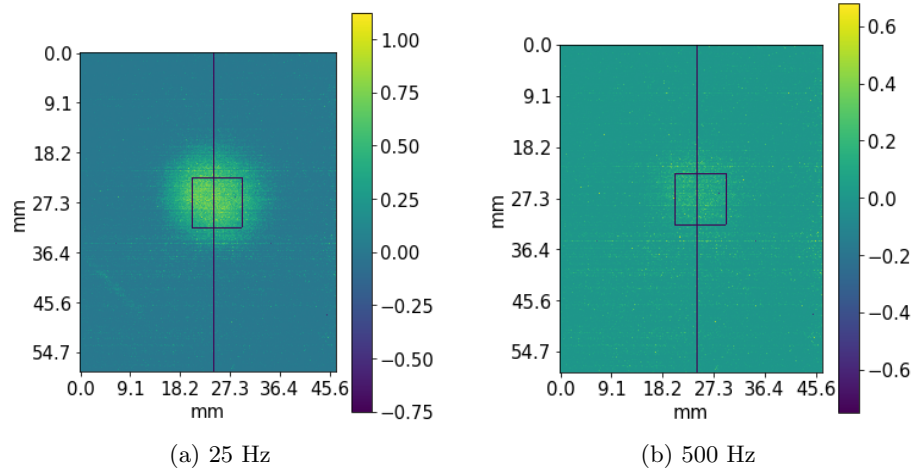


Figure 7: Averaged image in arbitrary units is shown for 25 Hz (a) and for 500 Hz (b). Along the vertical line a Gaussian was fitted. The intensity was also integrated over the square.

The valve was operated with a current of 40.4 A and a voltage of 39.2 V for the results we will present here. The helium pressure is set to 20 bar. For the discharge we used 150 V on the electronic supply voltage. The pulse length is set to 20 μ s.

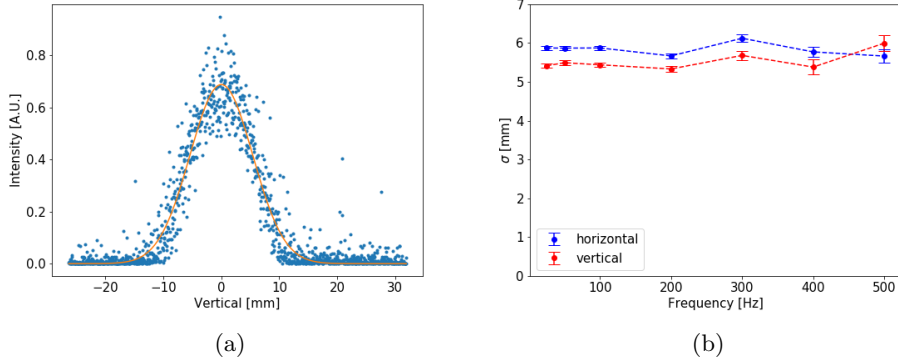


Figure 8: (a) A vertical cross section of the beam was taken and fitted to a Gaussian for 25 Hz. (b) Sigma as a function of the repetition rate.

In figure 7 the average image of the He^* beam for 25 Hz and 500 Hz is shown. A background image was taken beforehand and subtracted from all the images. In dark blue the vertical cross section as well as the area over which we integrated is marked. After the second skimmer the velocities of the metastable helium atoms follow a Maxwell-Boltzmann distribution. At distances much larger compared to the skimmer orifice the beam profile will approximately follow a Gaussian [5]. Figure 8a shows the vertical Gaussian fit for 25 Hz. The widths of the Gaussian is $\sigma_{25} = 5.42 \pm 0.05$ mm. In figure 8b sigma is shown as a function of the repetition rate. The width of the beam stays roughly the same for the different repetition rates. This is a good indication that the properties of the beam stay the same for higher repetition rates. The MCP is placed 73 ± 1 cm after the second skimmer. From this we calculated an opening angle of 0.458 ± 0.004 ° of the beam after the second skimmer. This gives a measure of the maximal dispersion of the beam.

We now concentrate on the individual images and no longer on an averaged image. Still the background was subtracted. The probability of measuring a given integrated intensity is shown in figure 9. We choose the same bin size for 25 Hz and 500 Hz. For 25 Hz there was no signal (red) in 60.66 % of the images and for 500 Hz in 69.75 %. The rest of the data (blue) again follows a Gaussian distribution which is centred around higher intensities for 25 Hz. The integrated intensity is proportional to the number of detected He^* atoms which again is proportional to the number of He^* atoms hitting the MCP. The probabilities of detecting metastable Helium atoms is shown

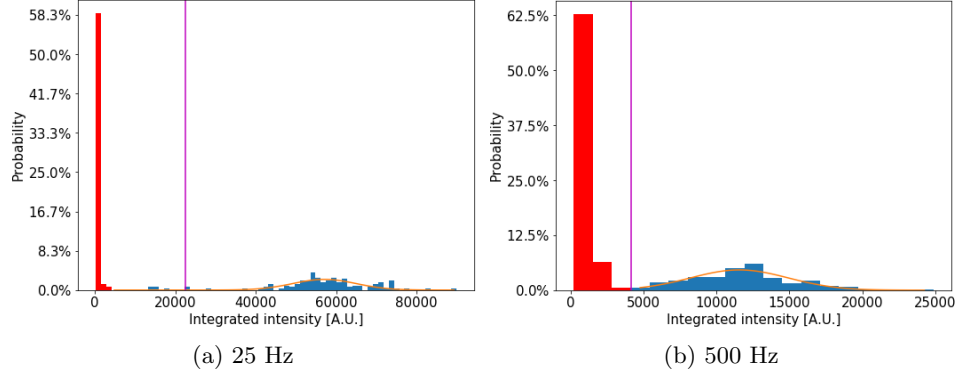


Figure 9: Fluctuations of integrated intensity for individual images in arbitrary units. Red counts as a fail and blue as success. The average integrated intensity for the given repetition rate is marked in magenta. Also shown is a Gaussian fit in orange.

in figure 10. The problem was not actually the detection but the discharge. The discharge failed more than half of the time and there were no metastable helium atoms to be detected. This was overcome by biasing the filament with a positive voltage of +20 V. The electrons are then accelerated towards the pinhole (grounded) and help with the discharge. The discharge then works all of the time.

Figure 11 shows the decrease of the integrated intensities with the repetition rate. All the lines are scaled to the same maximal value. The red line only considers successes (blue in the histograms like figure 9). The data for the green line was calculated from the voltage change on the MCP tracked by the oscilloscope ¹. The data from the MCP and the camera are in agreement. But lines clearly show a drop of the number of detected He* atoms as a function of the repetition rate. The source in the main setup usually runs with a repetition of 25 Hz. It was also tested for 100 Hz which already led to a reduction of the signal by 60 % [6]. The new source clearly does better than this.

We will now explain the reason for the reduction of the signal with the repetition rate. When the helium valve is operated at higher repetition rates it releases more gas into the source chamber in the same time. The vacuum pumps however still run at the same rate which leads to an increase

¹This data was acquired in collaboration with Pavel Stroganov.

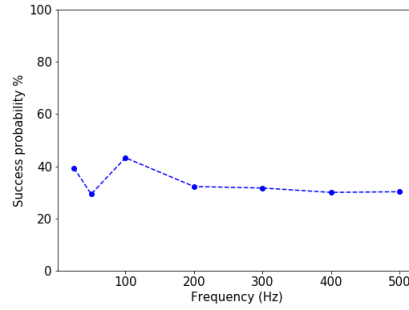


Figure 10: Probability of receiving a signal from He^* atoms hitting the MCP as a function of the repetition rate.

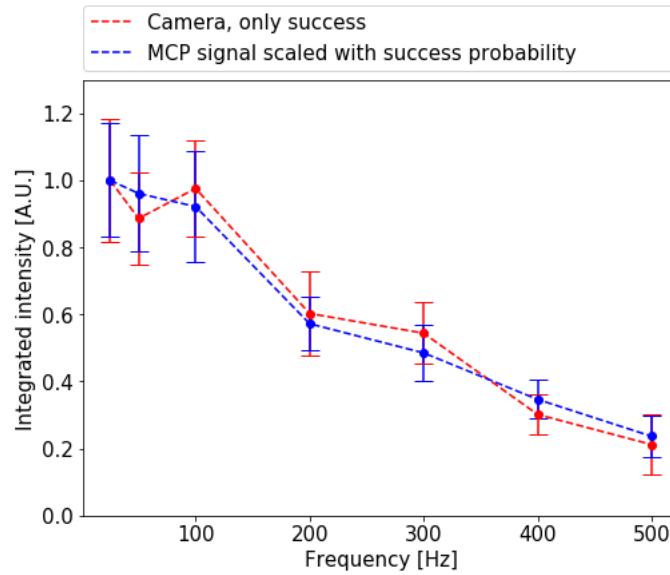


Figure 11: Intensities including their standard deviations for different repetition rates. The red curve is acquired from the images taken by the camera. Only images where He^* atoms were detected were taken into account. The blue curve was calculated from the data acquired by the oscilloscope.

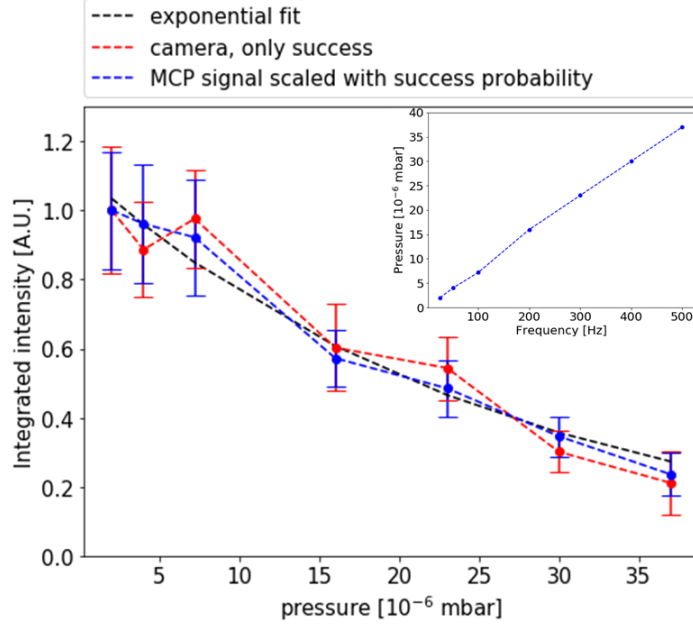


Figure 12: Integrated intensities as a function of the pressure in the source chamber as well as an exponential fit (black). The small plot in the top right corner shows the pressure in the source chamber for different repetition rates.

in pressure in the source chamber. This can be seen in the small plot in figure 12 for the different repetition rates. Due to the higher pressure in the source chamber more of the metastable helium atoms get deflected and never reach the MCP and we get less signal. We now also plot the integrated intensities as a function of the pressure. This together with an exponential fit (black) is shown in figure 12.

The ideal gas law $p = nk_B T$ gives the relationship between the pressure p , the Temperature in the source chamber T and the number density $n = N/V$. The collision probability can be written as

$$dp_c = ndV \quad (1)$$

With the infinitesimal volume $dV = \sigma v dt$. σ is the scattering cross section for Helium, v the velocity and t the time. The number of Helium atoms

change as follows

$$dN = -Ndp_c = -N \frac{p\sigma v}{k_B T} dt \quad (2)$$

The number of He* atoms therefore decays exponentially with the pressure.

$$N(t) = N_0 e^{-\frac{p\sigma v t}{k_B T}} \quad (3)$$

If we evaluate this at the first skimmer we get:

$$N_{skimmer} = N_0 e^{-\frac{p\sigma L_{skimmer}}{k_B T}} \quad (4)$$

$L_{skimmer} = 76$ mm is the distance between the valve and the first skimmer. This is smaller than in the main experiment, which makes the exponential drop slower. The measured pressure values were corrected by a gauge efficiency factor of 6 [1]. If we assume the beam particles to be at the same temperature as the environment ($T = 292$ K), we get a scattering cross section of $340 \pm 50 \text{ \AA}^2$ from the fit. In [7] the cross section for the scattering of metastable Helium from Helium atoms was measured to be $\sim 140 \text{ \AA}^2$. That value however was acquired for a velocity of 1000 ms^{-1} and the scattering gas was cooled down to 77.4 K. The difference can also arise due to the unknown effective temperature of the gas in our experiment or the anisotropy because of the supersonic expansion.

4 Conclusion and outlook

In the course of this semester project we have written a LabVIEW camera driver. The driver was then used to acquire the data presented in this thesis. There are however still many functionalities that could and probably will be added.

I have gained a first experience in working in an experimental environment and especially in how to deal with all the problems we have encountered. For me it was always hard to see the source of our problems but together with Sébastien we found all the leaks, burnt resistors, ... and finally got the source working.

The results presented in the last section show that we successfully produce He* atoms and can detect them on the MCP for repetition rates up to 500 Hz. This will make future experiments faster and reduces the signal-to-noise ratio

for a fixed measurement time. The integrated intensities fall of exponentially with the repetition rate. This is expected due to the rising pressure in the source chamber. In the data presented in the previous section the discharge failed more than half of the time. This issue could already by solved with a filament. The discharge now operates without problem.

References

- [1] T. S. Thiele, “Coherent manipulation of rydberg atoms close to surfaces at cryogenic temperatures,” Ph.D. dissertation, ETH Zurich, 2016.
- [2] D. Friese, “Towards continuous wave rydberg excitation for $2^3 s_1$ helium,” Master’s thesis, ETH Zurich, 2015.
- [3] J. Ladislav Wiza, “Microchannel plate detectors,” *Nuclear Instruments and Methods*, vol. 162, pp. 587–601, Jun. 1979.
- [4] “UI-3140CP Rev. 2,” September 15, 2017. [Online]. Available: <https://en.ids-imaging.com/store/ui-3140cp-rev-2.html>
- [5] M. Schulz-Weiling, H. Sadeghi, J. Hung, and E. Grant, “On the evolution of the phase-space distributions of a non-spherical molecular ultracold plasma in a supersonic beam,” *Journal of Physics B: Atomic, Molecular and Optical Physics*, vol. 49, no. 19, p. 193001, 2016. [Online]. Available: <http://stacks.iop.org/0953-4075/49/i=19/a=193001>
- [6] S. Garcia, “personal notes,” private communication.
- [7] E. W. Rothe, R. H. Neynaber, and S. M. Trujillo, “Velocity dependence of the total cross section for the scattering of metastable $he(3s1)$ by helium, argon, and krypton,” *The Journal of Chemical Physics*, vol. 42, no. 9, pp. 3310–3314, 1965. [Online]. Available: <http://dx.doi.org/10.1063/1.1696416>
- [8] “uEye .NET Manual 4.90,” September 15, 2017. [Online]. Available: https://en.ids-imaging.com/manuals/uEye.SDK/EN/uEye_DotNET_Manual_4.90/index.html

A LabVIEW Camera Driver Manual for UBS 3 CMOS Camera

Camera

The camera driver was written for an IDS UBS 3 CMOS camera. The model used is UI-3140CP-M-GL Rev.2.

Description

Most of the commands used in the LabVIEW camera driver are provided by IDS in a .NET library. It consists of several classes and methods. More information can be found on [8].

First the camera is initialized. This is done in the **SubVI_CameraInitParameters**. This SubVI also sets some parameters. Pixel clock and frame rate are set to the maximum value. These values (both in MHz) can be read from the indicators on the front panel. The gain is set to 100 which corresponds to a value of 1. The same is done for gamma.

The trigger mode can be chosen with the control on the front panel.

Then the area of interest (AOI) is set in the **SubVI_AOI**. The width and height as well as the x- and y-position can be chosen in the possible range. The maximum width is 1280 and the maximum height is 1024. The area of interest might influence the frame rate. Therefore the value of the frame rate is updated again.

The exposure is first set in the **SubVI_Exposure**. The possible values might also be affected by the area of interest.

SubVI_MemoryAllocation allocates memory for the chosen number of images to capture and the size of the AOI.

All these steps are done automatically when the VI starts to run.

If the “Acquire Background“ button is pressed a series of images will be taken and averaged. The image is displayed and automatically saved as .bin and .png in the selected folder. The filename will include the filename and the prefix Backg_ . The background image will then be subtracted from the

following images. To indicate this there is a round LED labeled “Subtract background “ that will glow green.

The acquisition starts when the “Acquire“ button is pressed. Number of images to capture indicates how many pictures will be taken. There is a progress bar (“Progress %“) which indicates how many pictures have already been taken. If this takes too long the loop will time out after the given TimeOut [s]. The data will be averaged in **SubVI_Average** and if previously there was a background image taken it will be subtracted. **SubVI_ArrayToImage** makes it possible to display an image. All the images and the averaged one can also be saved. There are two switches (“Save Average“ and “Save All“) to do so. The averaged image will be saved with the prefix Av_ and the single images with All_ and a filename. The saving is done in **SubVI_Save** and **SubVI_SaveAll**. To save all the images takes some time and the progress is traced by the “Saving Progress %“ bar. After this one can acquire a new series of images by pressing “Acquire“ again. It is also possible to change one or more parameters.

If there is a value change in Number of to capture the memory will be freed by **SubVI_FreeMemory** and new memory will be allocated in **SubVI_MemoryAllocation**.

It is also possible to change the exposure and the trigger mode.

If any of the parameters of the area of interest is changed the memory will also be freed and new memory allocated. The pixel clock and the frame rate are set to the maximum possible value again and the exposure is also updated.

If the “Exit“ button is pressed the memory will be freed and the camera is exited.



Declaration of originality

The signed declaration of originality is a component of every semester paper, Bachelor's thesis, Master's thesis and any other degree paper undertaken during the course of studies, including the respective electronic versions.

Lecturers may also require a declaration of originality for other written papers compiled for their courses.

I hereby confirm that I am the sole author of the written work here enclosed and that I have compiled it in my own words. Parts excepted are corrections of form and content by the supervisor.

Title of work (in block letters):

INVESTIGATING HIGH REPETITION RATES FOR A METASTABLE HELIUM SOURCE

Authored by (in block letters):

For papers written by groups the names of all authors are required.

Name(s):

DUETSCHLER

First name(s):

ALISHA

With my signature I confirm that

- I have committed none of the forms of plagiarism described in the '[Citation etiquette](#)' information sheet.
- I have documented all methods, data and processes truthfully.
- I have not manipulated any data.
- I have mentioned all persons who were significant facilitators of the work.

I am aware that the work may be screened electronically for plagiarism.

Place, date

ZURICH, 10.09.17

Signature(s)

For papers written by groups the names of all authors are required. Their signatures collectively guarantee the entire content of the written paper.